Tunable Twisting Motion of Organic Linkers via Concentration and Hydrogen-Bond Formation

Tunable Twisting Motion of Organic Linkers via Concentration and Hydrogen-Bond Formation

Ahmed M. El-Zohry[a], Abdullah Alturki[a], Jun Yin[a], Arijit Mallick[b], Osama Shekhah[b], Mohamed Eddaoudi[b], Boon S. Ooi[c], and Omar F. Mohammed[a]*

[a] King Abdullah University of Science and Technology (KAUST), Division of Physical Sciences and Engineering, Thuwal 23955-6900, KSA.

[b]Functional Materials Design, Discovery and Development Research Group (FMD3), Advanced Membranes and Porous Materials Center (AMPMC), Division of Physical Sciences and Engineering (PSE), King Abdullah University of Science and Technology (KAUST), Thuwal 23955-6900, KSA.

[c] Photonics Laboratory, King Abdullah University of Science and Technology (KAUST), Thuwal 23955-6900, KSA.

*omar.abdelsaboor@kaust.edu.sa (O.F.M)

Abstract

Benzothidiazole dibenzoic acid derivative (BTDB) is a well-known organic linker in various metal-organic framework structures as well as a fluorescent probe in biological systems. Here, we demonstrate that the radiative and non-radiative decay channels of BTDB can be interplayed and precisely controlled through concentration and hydrogen bond interactions as directly evidenced experimentally and theoretically. This leads to excited-state structural changes that significantly suppress the torsional motion around the Benzothidiazole moiety, leading to an enormous increase in the emission quantum yields from ~1% to 70%. These changes are associated with the existence of two equilibria where dimers and small-oligomers form in dimethylformamide (DMF), with high formation constants of 18,000 M^{-1} and 1.2×10^{13} M^{-3}, respectively. These evolving species, i.e., the dimers and oligomers, are formed via hydrogen bonds between carboxylic acid groups present at the far-edge of the rod-like BTDB molecules. The estimated repeating number for this small-oligomer formation via bonded monomers is eight in DMF, as shown by emission spectra analysis. With deprotonation as a control experiment, these associated species can easily collapse to the initial monomer species, confirming the role of the hydrogen-bond formation on the observed phenomena. Theoretical studies and NMR experiments not only confirm the existence of the dimers, but also demonstrate the important role of the hydrogen bonds on the excited-state dynamics. These new findings provide a better understanding of the photophysical behaviors of organic linkers used in a wide range of chemical and biological applications.

Introduction

Organic molecules have an enormous range of applications in various fields such as fluorescent probes,[1] photovoltaics[2-3], transistors[4], supramolecular electronics[5], white-light generation[6-7], and metal-organic frameworks (MOFs).[8-10] Many fundamental photophysical and photochemical properties of organic molecules including charge transfer, charge separation and charge recombination are well understood in several chemical systems using time-resolved laser spectroscopy.[1, 11-14] On the other hand, most of those organic molecules exhibit very low photoluminescence quantum yields (PLQY) especially in liquid phase, depending on the active non-radiative deactivation channels present such as torsional/twisting motions, excited state structural changes and ultrafast internal conversion.[15-19] For instance, torsional motions are commonly known as a very efficient non-radiative deactivation mechanisms for organic molecules upon photon-excitation in a wide range of fields including biological and chemical systems as well as solid-state photovoltaic materials.[18-28] It should be pointed out that torsional or twisting motions can lead to cis-trans isomerization process, twisted-intramolecular charge transfer, and population of conical intersections due to the strong electronic coupling between the ground and excited state levels.[17-18, 23-24, 29-30] All these evolving photoinduced processes can be very beneficial in many research areas of significance including protein relaxation[20] and DNA protection.[31] They can also be detrimental and crucial steps in solar cells applications.[18-19] However, torsional motions, on the other hand, can lead to ultrafast deactivation of the excited state molecules and strongly compete with other processes such as product formation and radiative recombination processes.[21]

To significantly suppress such non-radiative twisting motions and subsequently enhance the fluorescence quantum yields of such organic molecules, several chemical and material approaches have been established and developed, such as forming aggregation/suspensions at relatively high concentration in the presence of solvent mixtures, producing solid-state forms, constructing thin-films, incorporating heavy metal atoms, and embedding them in polymer chains.[15-16, 32-33] Nevertheless, these new approaches can induce other nonradiative processes, such as energy transfer, charge transfer, and defect states, that lead to different deactivation pathways of the excited state of the targeted molecules.[1, 11, 18, 30, 34-47]

In this paper, we show for the first time that relatively low concentrations (nano- to micromolar scale) of a soluble organic linker with double carboxylic groups can form distinct species with

different emission peaks, different excited state lifetimes, and exceptionally high PLQYs. The evolving species are formed through hydrogen bonds at the carboxylic acid of the organic linker. The presence of distinct species at different concentrations is fully supported by theoretical calculations and various spectroscopic experiments including steady-state absorption and emission spectra, lifetime measurements, PLQY, and NMR. These species include dimers and small-oligomers, with high formation constants for both species. The organic molecule used herein is Benzothidiazole dibenzoic acid derivative (BTDB), which is commonly used as a linker in MOF synthesis[48-49] and as a fluorescent probe in biological applications due to its high π-conjugation, molar extinction coefficient, and high photostability.[50] The outcome of this study reveals simple and novel approaches to obtain high PLQY and tunable emission spectral ranges in the liquid phase by optimizing the structural design of organic molecules.

Experimental Section:

Dimethylformamide (DMF), ethanol (EtOH), and Tetrahydrofuran (THF) were purchased from Aldrich, and used without further purification. The synthesis procedure for the linker 4,4′-(benzoic]i1,2,5]thiadiazole-4,7-diyl) dibenzoic (BTDB) is shown in the supporting information along with the NMR data; see Figure S1 and Figure S2. The organic linker purity was confirmed by mass spectrum and thin layer chromatography (TLC) tests, as well as the steady-state absorption and emission spectra of the starting materials, as shown in Figure S3 and Figure S4. Details about steady-state, time resolved measurements, and density functional theory calculations are found in the supporting information.

Results and Discussion

Figure 1A shows the normalized absorption spectra for the BTDB linker at concentrations of 3-1000 μM in DMF (see the chemical structure of BTDB in the inset of Figure 1A). With increasing BTDB concentration, a slight blue spectral shift of ca. 12 nm is observed in the S_1 band, where 3 μM has an absorption maximum of 390 nm, and the highest concentration reaches a maximum of 378 nm. It should be noted that the S_2 absorption band is slightly red-shifted with 4 nm in the same range of concentration. In contrast, the corresponding concentrations show dramatic changes in the emission spectra upon 380-nm excitation light (Figure 1B). At a low concentration of 0.1 μM, a broad emission peak at 485 nm is observed. The emission peak systematically intensifies and broadens at 3 μM, then splits into two distinctive emission peaks located at 420 nm and 620 nm at

64 μM (Figure 1B). To rule out solvent contribution for the spectral changes with concentration, various solvents with different properties were tested such as DMSO, EtOH, and THF, and similar emission trends are observed (see Figure S5). Such spectral changes in absorption and emission measurements could be attributed to aggregation or dimerization equilibrium.[18, 51] Thus, density functional theory (DFT) calculations were performed to clarify the origin of the spectral changes. The DFT results show a calculated absorption spectrum of BTDB molecules in DMF with two excited states at 412 and 320 nm (Figure 1C). For the lowest excited state transition, S_1, the electronic densities in the ground and excited states, HOMO and LUMO, show similar distributions with an optimized dihedral angle for the ground state geometry of ca. 37.5° present around the Benzothidiazole moiety; see Figure 1C and Figure S6. The calculated emission spectrum shows an emission maximum of 535 nm with an optimized dihedral angle of ca. 18.2°; see Figure 1D. The change in the dihedral angle with the observed calculated Stock's shift of ca. 5580 cm^{-1} highlights the role of torsional processes such as isomerization and twisting motions in relaxing/deactivating the excited state of BTDB, as shown previously for other organic dyes.[17-19, 21-22, 24]

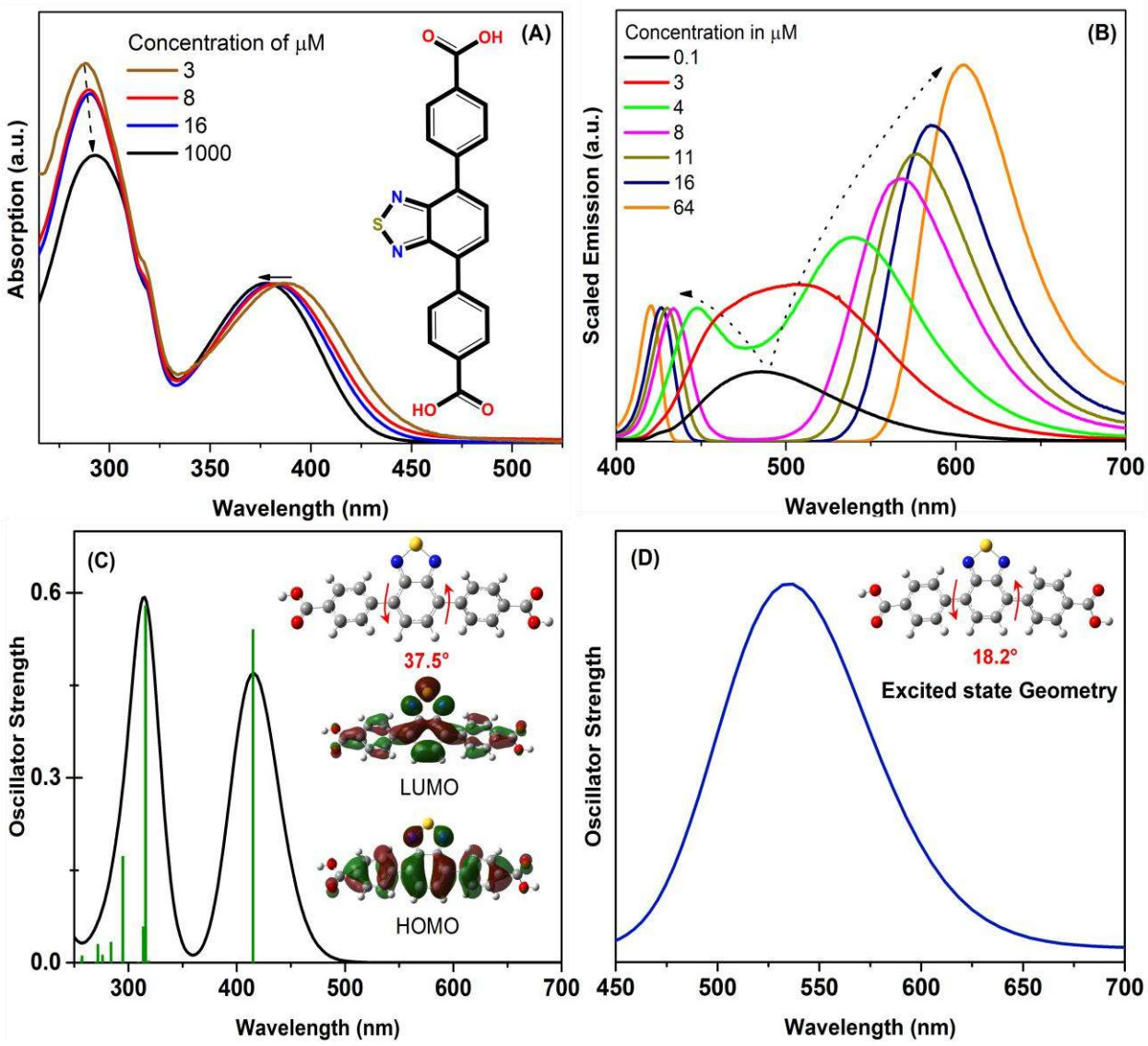

Figure 1: (A) Normalized absorption spectra of BTDB linker in DMF at various concentrations with the linker chemical structure inside. (B) Scaled emission spectra of linker in DMF at a low range of concentrations (0.1-64 μM) showing the splitting of the emission band into two emissive states at two different energy levels, representing the first equilibrium; see text for more information. (C) Calculated absorption spectrum of BTDB molecule in DMF with the optimized dihedral angle structure in the inset. The optimized electronic distributions of the ground and excited states are shown in the inset, HOMO and LUMO. (D) Calculated emission spectrum of BTDB molecules in DMF with the excited state geometry in the inset, showing an optimized dihedral angle of 18.2°.

For further correlation between the calculated emission and the dihedral angle, Figure S7 shows the dependence of the emission maximum on the variation of the dihedral angle around the Benzothidiazole moiety, where angles larger than the optimized angle value show blue shifted emission spectra. This result highlights the dependence of the emission maxima on the thermalized dihedral angle. To differentiate between the aggregation and dimerization equilibria, two possible

structures of BTDB were optimized through DFT along with their calculated emission spectra. Figure 2 shows the possible aggregation structure due to parallel π-π stacking of two molecules of BTDB and a possible dimer structure through hydrogen bonds at the carboxylic acid groups between two monomers. The emission spectrum calculated for the aggregate form has a blueshifted spectrum of ca. 60 nm with respect to the monomer case (Figure 2). Nevertheless, the dimer form presents two emission peaks with similar trends to those observed in the experimental data; see Figure 1B and Figure 2. Interestingly, the optimized dihedral angle in the dimer form is different from the monomer case, which indicates a change in the excited state lifetime and the emission quantum yield, as shown in a later section. Also, it is worth mentioning that the slight increase in oscillator strength upon dimerization could be attributed to the increase in the probability of excited electrons to switch back to the orbitals in the ground state because of various molecules and their orbitals are close to each other upon dimerization.

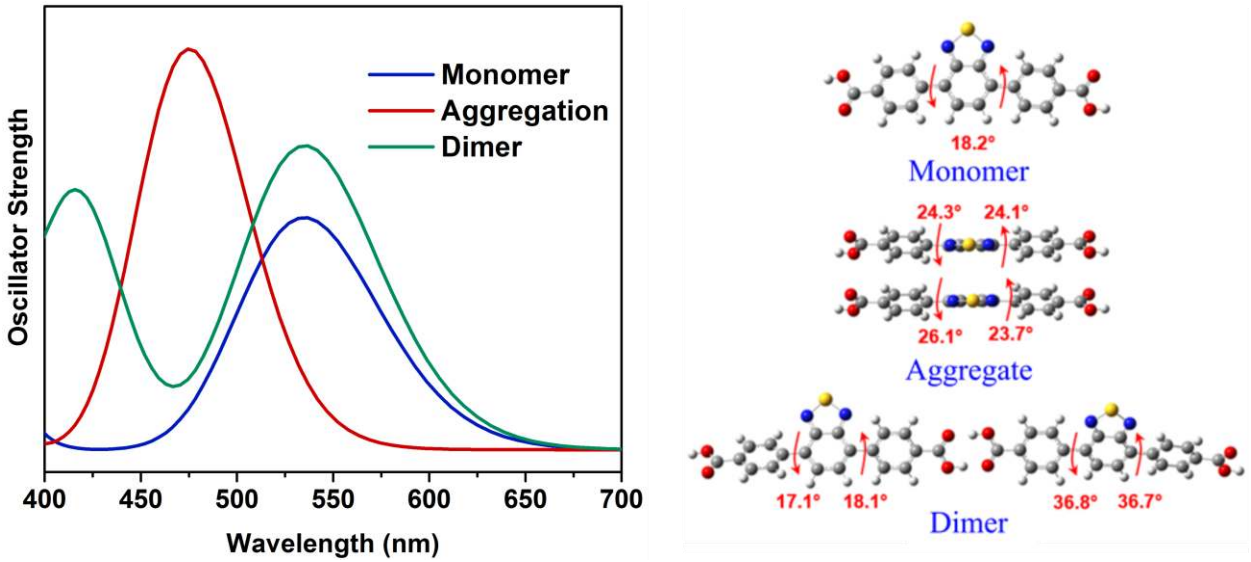

Figure 2: Calculated emission spectra of BTDB monomer, aggregated form and dimer in DMF solvent with their optimized dihedral angles to the right side.

Beyond the 64 μM concentration, the emission spectra evolve further, with the two distinctive emission peaks approaching each other and eventually merging into one broad peak centered at 480 nm at a concentration of 1.0 mM (Figure 3A). These emission spectral changes with concentration from 0.1 to 1000 μM could be attributed to the presence of two equilibrium constants. We postulate that the first equilibrium is for dimer formation in the concentration range of 0.1-64 μM. Then, at a higher concentration range, another equilibrium is present where the

dimers form a small size "*oligomer*"-like structure. The following equations represent these proposed mechanisms, where M, D and O represent monomers, dimer, and oligomer species, respectively, K_{eq}^{O} is the oligomer formation constant, and I_{em}^{O} is the oligomer emission at a specific wavelength:

$$M + M \overset{K_{eq}^{D}}{\longleftrightarrow} D$$

The monomer-dimer equilibrium constant K_{eq}^{D} equals:

$$K_{eq} = \frac{[D]}{[M]^2} \quad \text{.....(1)}$$

The total concentration of BTDB in solution, C_0, can be expressed as follows[35, 40, 42, 52]:

$$C_0 = [M] + 2[D] \text{.....(2)}$$

The total emission intensity, I_{em}^{total}, is the sum of the emission of the monomer (I_{em}^{M}) and the dimer (I_{em}^{D}) normalized to their fractional concentrations in solution:

$$I_{em}^{total} = I_{em}^{M} \frac{[M]}{C_0} + I_{em}^{D} \frac{2[D]}{C_0} \text{.....(3)}$$

By solving equations 1, 2, and 3 together, the following expression can be obtained:

$$I_{em}^{total} = (I_{em}^{M} - I_{em}^{D}) \frac{2}{(\sqrt{8K_{eq}C_0+1}+1)} + I_{em}^{D} \text{.....(4)}$$

By using the nonlinear least squares fitting method with equation 4 and knowing the total concentration and the total emission intensity at 680 nm, the dimer formation constant is found to be 18,000 M^{-1} (see Figure 3B). Such a high equilibrium constant has been reported previously for carboxylic dyes.[35]

Similarly, at higher concentrations, the dimers tend to form small-sized oligomers. In this case, the following equation can be used:

$$nD \overset{K_{eq}^{P}}{\longleftrightarrow} O \text{.....(5)}$$

where n is the number of dimer species needed to form one small size oligomer, which cannot be estimated from our experiments. By repeating the same derivation for the dimer formation, the

following equation is derived and relates the total emission intensity to the concentration used at the higher concentration range:

$$I_{em}^{total} = (I_{em}^{D} - I_{em}^{O}) \frac{1}{(nK_{eq}[C_0/(n+1)]^{n-1}+1)} + I_{em}^{O} \quad \text{.....(6)}$$

Considering the assumption that $[D] = C_0/(n+1)$, the absorptivity is unchanged at this concentration regime (32 µM-1 mM); see Figure S8. Equation 6 fits the extracted data for the oligomer formation well, with an *n* parameter of ca. 4, and a formation constant of ca. 1.2×10^{13} M^{-3} (Figure 3B). This result means that at least four dimers need to bind together to form the small oligomer with the characteristic emission spectrum through hydrogen bonds.

Additionally, DFT calculations show that by increasing the number of associated monomers through hydrogen bonds until a tetramer is formed, the calculated double emission peaks start to change, and one emission peak minimizes while the other maximizes; see Figure S9. Thus, with eight associated monomers, only one broad emission peak predominates, as shown experimentally. In addition, H-NMR measurements of BTDB at concentrations of 64 µM and 1000 µM demonstrate this result as well the change of the hydroxyl group environment at the carboxylic acid, where the FWHM increases from 0.084 ppm to 0.144 ppm in the aforementioned concentrations due to extensive hydrogen bonding interactions; see Figure S10. To the best of our knowledge, this is the first reported emission data for the formation of dimers and small oligomers from dissolved small organic molecules at such low concentrations.

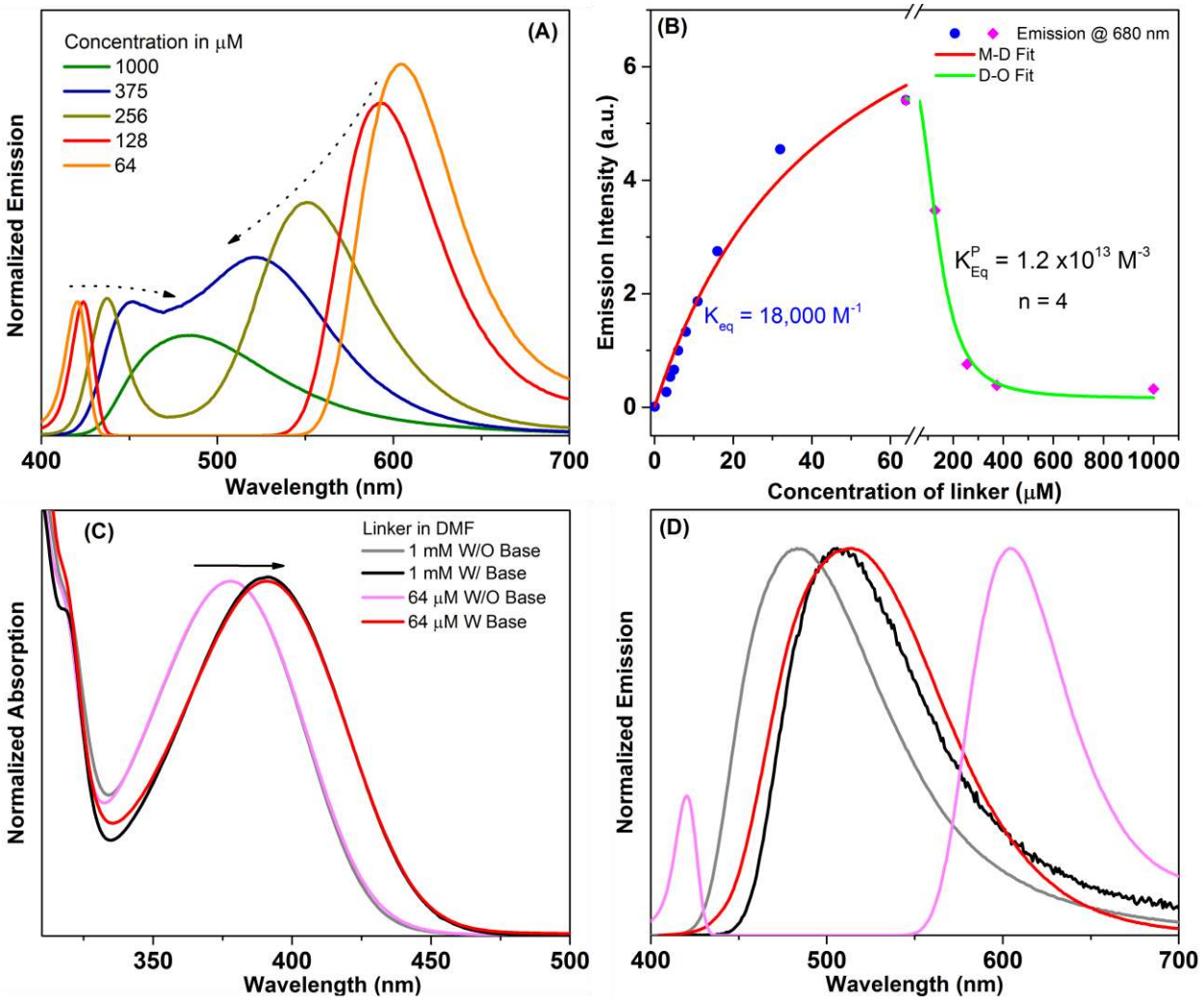

Figure 3: (A) Scaled emission spectra of linker in DMF at higher range of concentrations (64-1000 μM) showing the merging of two emission bands into one emissive state at intermediate energy level, representing the existence of the second equilibrium; see text. (B) Plots of total emission intensity at 680 nm versus the concentration of BTDB organic molecules in DMF with the fittings obtained. Using equations 4 & 6, the formation constants for the dimer and oligomer species can be extracted. (C) Normalized absorption spectra of 64 μM and 1 mM of linker in DMF in the absence and presence of organic base. (B) Scaled emission spectra of 64 μM and 1 mM of linker in DMF in the absence and presence of organic base with scaled emission from 0.1 μM, showing the similarities of emission from different concentrations with the addition of organic base. Legend is shown in the inset of (D). The excitation was 380 nm.

The mechanism proposed herein for dimerization and oligomerization depends on the existence of carboxylic groups at both sides of the molecule, making them capable of reaching up to four attached dimers, "eight monomers", when forming this small soluble oligomer, as shown in Figure 3B. Dimerization through carboxylic acids has been discussed previously in the literature for molecules with one carboxylic group.[35, 42] Carboxylic acids tend to associate by forming hydrogen

bonds between their hydroxyl and ketone groups. However, most of the molecules investigated have small dimerization constants[41], with rare exceptions that have high dimerization values.[35] The capability of BTDB dye molecules to form such long chains through hydrogen bond formation stems from the presence of two carboxylic acid groups at the two ends of the rod-like molecules, as shown in the structure in Figure 1. To further prove the contribution of the hydrogen bond to the BTDB behavior, an organic base (diethyl amine) was added to two different concentrations of BTDB, 64 µM and 1.0 mM, corresponding to the dimers and oligomers, respectively. The organic base tends to deprotonate the carboxylic group present in the BTDB. Both the absorption and emission spectra of the two concentrations transformed into the corresponding spectra of the monomer, as shown in Figure 3C-D, confirming the contribution of hydrogen-bond formation through carboxylic acid groups to the formation of dimers and small oligomers of BTDB in solution. Additionally, the ester form of the BTDB molecules (see Figure S1) has the same emission spectra at the same working range of concentrations from 0.1 µM to 1 mM, illustrating the importance of carboxylic acid on the observations seen herein; see Figure S11.

Moreover, BTDB species have different excited state dynamics. Figure 4A shows the time-resolved photoluminescence (TRPL) kinetics of BTDB at various states of different concentrations, 0.1 µM (monomers), 64 µM (dimers), and 1 mM (small-sized oligomer). All the kinetics could be fitted via a global fitting procedure using exponential decay equations, giving one primary component of 8.3 ns with different amplitudes for each species (Table 1). The oligomer concentration at 1 mM shows only single exponential decay of 8.3 ns. By decreasing the concentration to 64 µM, for the dimer species, fitting the emission decays at 420 nm and 660 nm shows similar trends, with the lifetime of the primary component ca. 5 ns and a shared lifetime of 8.3 ns; see **Table 1**. The presence of at least two forms of dimers is also verified by collecting excitation spectra at each emission wavelength, 420 and 580 nm, where two excitation spectra are found, indicating different geometries of dimer species in the ground state prior to excitation; see **Figure 4B**. Interestingly, the low concentration of 0.1 µM that presumably corresponds to the monomer species shows a fast emission decay with a dominant lifetime of 0.95 ns; see Table 1. Nevertheless, even at such low concentration, a minority of dimer species are present, which is reflected in the blue shift observed in the emission spectra at lower concentrations; see Figure S12.

The photoluminescence quantum yield (PLQY) measurements show a consistent trend with the emission lifetime measurements, as shown in Table 1. A low PLQY value for the monomer species (~ 1.2%) and a higher one for the oligomer species (~ 69%) were measured (see Table 1 and Figure S13). These data emphasize that monomer species have at least one dominant nonradiative decay channel, minimizing the PLQY and emission lifetime. In contrast, upon increasing the concentration and consequentially forming the dimer and oligomer species, this nonradiative channel is significantly suppressed, increasing the amplitude of the longer lifetime, 8.3 ns, as well as the PLQY (Table 1). One possible nonradiative decay channel is the presence of isomerization or torsional motion in the excited state, which has been observed for similar organic molecules, making the excited state lifetime shorter with low PLQY.[17-19, 53] To suppress such channels, plastic polymer matrix (PMMA) was used with BTDB at various concentrations; see Figure 4C. Across all the concentrations, the use of PMMA makes the emission spectra and the lifetime similar to those of the oligomer; see Figure 4D. This result confirms the contribution of torsional processes to the excited state and the PLQY. Thus, PMMA suppresses the torsional motion present in the monomer species with similar mechanisms as those in the oligomerization process. Also, the disappearance of double emission peaks for 64 μM observed in solution, when embedded in PMMA, highlights the contribution of excited state torsional motions prior to emission in liquid phase.

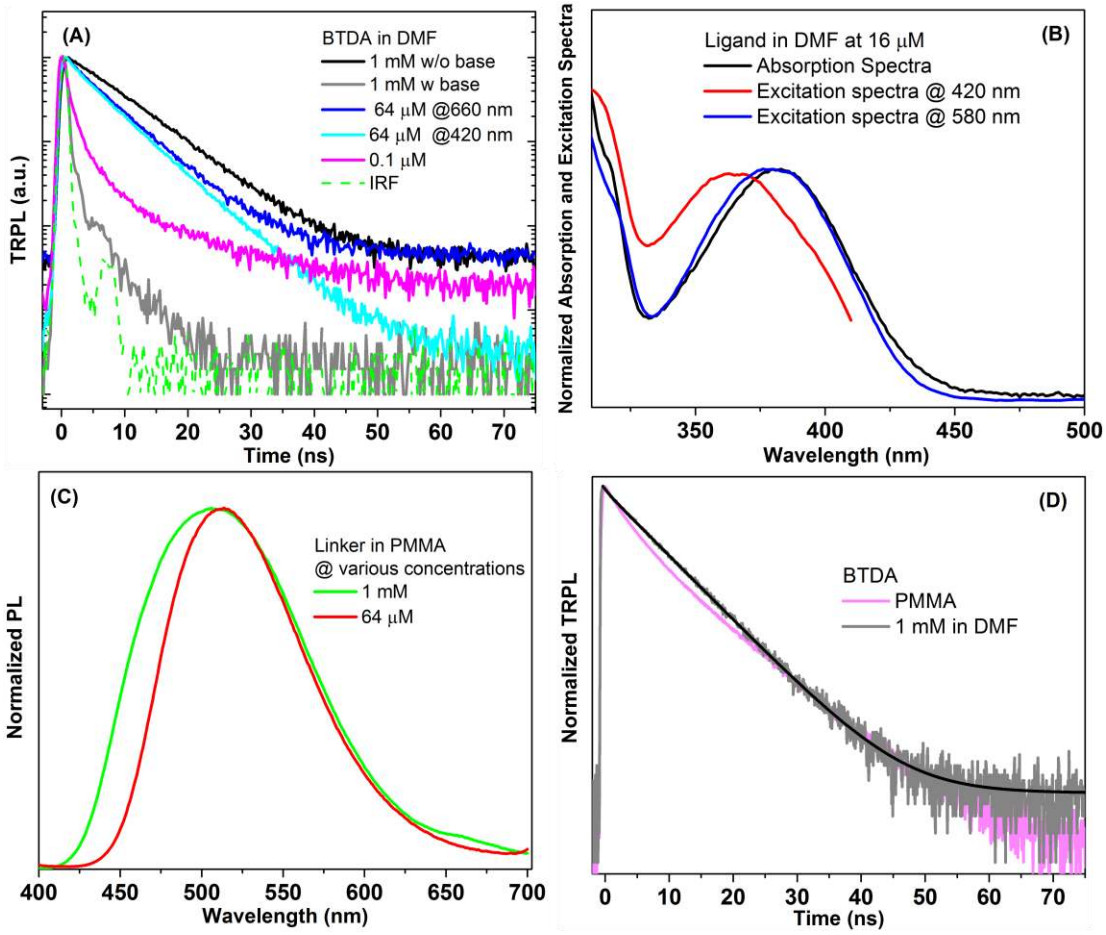

Figure 4: (A) Normalized time-resolved emission for linker in DMF at various concentrations, IRF ~500 ps, excitation wavelength was 400 nm. (B) Normalized time-resolved emission for linker in DMF at low concentrations and two different emission wavelengths as shown in the legend. (C) Normalized emission spectra of linker in PMMA at various concentrations showing one emissive band. (D) TRPL for linker in DMF with 1 mM concentration and low concentration embedded in PMMA.

In addition, the DFT calculations show that dimer, trimer, and tetramer species have similar extended dihedral angles to those of the monomer species in the ground state, illustrating that these species formed in the excited state suppress the torsional motion around the Benzothidiazole moiety shown for the calculated geometry for the excited monomer; see Figure 1, Figure 2, and Figure S9.

Table 1: Photophysical properties of BTDB species at different concentrations with the emission fitting parameters from global fit using the exponential equation $A_1e^{-t/\tau 1} + A_2e^{-t/\tau 2}$. The excitation wavelength was 380 nm.

Concentration (μM)	Emission wavelength (nm)	Quantum yield (Φ) (%)	Emission lifetimes, ns (amplitude %)	
			τ_1 (%)	τ_2 (%)
0.1	----	1.2 ±0.8	0.95 (94)	8.3 (6)
64 (dimer 1)	420	58 ±2.1	4.7 (66)	8.3 (34)
64 (dimer 2)	660		5.3 (72)	8.3 (28)
1000	----	69 ±3	---	8.3 (100)
1000 with base	----	1.6 ±1	0.6 (99)	8.3 (1)

All the excited state processes observed for the BTDB molecules in DMF can be summarized as follows. With excitation of the monomer species at low concentration, the molecule is thermalized and emits light at approximately 480 nm. However, for the excited monomer state, an active nonradiative channel leads the excited molecule to reach a conical intersection through large torsional motion around the Benzothidiazole moiety. This active conical intersection leads to low PLQY (~1-2%) and short excited state lifetime. Upon dimerization through hydrogen bonds, the potential energy surface in the excited state appears to change; the conical intersection is weakly active, leading to double thermalized states with two emission wavelengths at 420 and 620 nm, possibly due to different forms of dimers. The high PLQY in the dimer concentration range, ~58%, is likely due to presence of other species such as trimer, tetramer, or oligomer species at low concentrations. In the oligomer case or in PMMA, the two excited energy minima merge into one energy minimum where the excited state has a high activation energy for torsional motions, leading to central emissions at 480 nm with a high PLQY (~70%).

Conclusions

In this work, we demonstrate for the first time how simple organic linkers terminated with carboxylic acid groups can associate through hydrogen-bond formation at low concentrations, creating dimer and small oligomer species that have very distinct emission properties. We have also found that these dimers and oligomers exhibit almost 70 times higher emission quantum yields than that of the monomer. This result could be attributed to a significant reduction of the nonradiative-decay channels due to the suppression of twisting motions around the Benzothidiazole moiety as shown theoretically and experimentally. This study opens new frontiers

for deep understanding of the photophysical behaviors of organic linkers commonly used in a wide variety of chemical and biological applications. In addition, we show that highly emissive organic molecules can be obtained in liquid phase at considerably low concentrations with optimized molecule structure.

Supplemental Information Description

The supporting information contains information about the instrumentations used in details and the synthetic procedure used for the organic linker. Supplementary figures from S1 to S13 and are also provided.

Acknowledgements

The research reported in this publication was supported by funding from King Abdullah University of Science and Technology (KAUST). Thanks to Dr. Jafar Khan for helpful discussions.

References

1. Stennett, E. M. S.; Ciuba, M. A.; Levitus, M., Photophysical Processes in Single Molecule Organic Fluorescent Probes. *Chem. Soc. Rev.* **2014**, *43*, 1057-1075.
2. Kaur, N.; Singh, M.; Pathak, D.; Wagner, T.; Nunzi, J. M., Organic Materials for Photovoltaic Applications: Review and Mechanism. *Synthetic Met.* **2014**, *190*, 20-26.
3. Xu, L.; Wang, J.; Villa, M. d. A.; Daunis, T. B.; Lee, Y. J.; Malko, A. V.; Hsu, J. W. P., Quantitative Analyses of Competing Photocurrent Generation Mechanisms in Fullerene-Based Organic Photovoltaics. *J. Phys. Chem. C* **2016**, *120*, 16470-16477.
4. Kumar, B.; Kaushik, B. K.; Negi, Y. S., Organic Thin Film Transistors: Structures, Models, Materials, Fabrication, and Applications: A Review. *Polym. Rev.* **2014**, *54*, 33-111.
5. Molla, M. R.; Gehrig, D.; Roy, L.; Kamm, V.; Paul, A.; Laquai, F.; Ghosh, S., Self-Assembly of Carboxylic Acid Appended Naphthalene Diimide Derivatives with Tunable Luminescent Color and Electrical Conductivity. *Chem. Eur. J.* **2014**, *20*, 760-771.
6. Malakar, P.; Modak, D.; Prasad, E., Pure White Light Emission from Organic Molecules Using Solvent Induced Selective Self-Assembly. *Chem. Comm.* **2016**, *52*, 4309-4312.
7. Zhao, J. Z.; Ji, S. M.; Chen, Y. H.; Guo, H. M.; Yang, P., Excited State Intramolecular Proton Transfer (ESIPT): From Principal Photophysics to the Development of New Chromophores and Applications in Fluorescent Molecular Probes and Luminescent Materials. *Phys. Chem. Chem. Phys.* **2012**, *14*, 8803-8817.
8. Cui, Y. J.; Chen, B. L.; Qian, G. D., Lanthanide Metal-Organic Frameworks for Luminescent Sensing and Light-Emitting Applications. *Coordin. Chem. Rev.* **2014**, *273*, 76-86.
9. Kitagawa, S., Metal–Organic Frameworks (MOFs). *Chem. Soc. Rev.* **2014**, *43*, 5415-5418.
10. Gutierrez, M.; Sanchez, F.; Douhal, A., Spectral and Dynamical Properties of a Zr-Based MOF. *Phys. Chem. Chem. Phys.* **2016**, *18*, 5112-5120.

11. Qian, H.; Cousins, M. E.; Horak, E. H.; Wakefield, A.; Liptak, M. D.; Aprahamian, I., Suppression of Kasha's Rule as a Mechanism for Fluorescent Molecular Rotors and Aggregation-Induced Emission. *Nat. Chem.* **2016**, *9*, 83-87.
12. Mohammed, O. F.; Kwon, O. H.; Othon, C. M.; Zewail, A. H., Charge Transfer Assisted by Collective Hydrogen-Bonding Dynamics. *Angew. Chem. Int. Edit.* **2009**, *48*, 6251-6256.
13. Mohammed, O. F.; Adamczyk, K.; Banerji, N.; Dreyer, J.; Lang, B.; Nibbering, E. T. J.; Vauthey, E., Direct Femtosecond Observation of Tight and Loose Ion Pairs Upon Photoinduced Bimolecular Electron Transfer. *Angew. Chem. Int. Edit.* **2008**, *47*, 9044-9048.
14. Mohammed, O. F.; Banerji, N.; Lang, B.; Nibbering, E. T. J.; Vauthey, E., Photoinduced Bimolecular Electron Transfer Investigated by Femtosecond Time-Resolved Infrared Spectroscopy. *J. Phys. Chem. A* **2006**, *110*, 13676-13680.
15. Mei, J.; Leung, N. L. C.; Kwok, R. T. K.; Lam, J. W. Y.; Tang, B. Z., Aggregation-Induced Emission: Together We Shine, United We Soar! *Chem. Rev.* **2015**, *115*, 11718-11940.
16. Hong, Y. N.; Lam, J. W. Y.; Tang, B. Z., Aggregation-Induced Emission. *Chem. Soc. Rev.* **2011**, *40*, 5361-5388.
17. El-Zohry, A. M.; Roca-Sanjuan, D.; Zietz, B., Ultrafast Twisting of the Indoline Donor Unit Utilized in Solar Cell Dyes: Experimental and Theoretical Studies. *J. Phys. Chem. C* **2015**, *119*, 2249-2259.
18. El-Zohry, A.; Orthaber, A.; Zietz, B., Isomerization and Aggregation of the Solar Cell Dye D149. *J. Phys. Chem. C* **2012**, *116*, 26144-26153.
19. Zietz, B.; Gabrielsson, E.; Johansson, V.; El-Zohry, A. M.; Sun, L.; Kloo, L., Photoisomerization of the Cyanoacrylic Acid Acceptor Group–a Potential Problem for Organic Dyes in Solar Cells. *Phys. Chem. Chem. Phys.* **2014**, *16*, 2251-2255.
20. Usman, A.; Mohammed, O. F.; Nibbering, E. T. J.; Dong, J.; Solntsev, K. M.; Tolbert, L. M., Excited-State Structure Determination of the Green Fluorescent Protein Chromophore. *J. Am. Chem. Soc.* **2005**, *127*, 11214-11215.
21. Rosspeintner, A.; Lang, B.; Vauthey, E., Ultrafast Photochemistry in Liquids. *Annu. Rev. Phys. Chem.* **2013**, *64*, 247-271.
22. Lin, Y. D.; Chow, T. J., Geometrical Effect of Stilbene on the Performance of Organic Dye-Sensitized Solar Cells. *J. Mater. Chem.* **2011**, *21*, 14907-14916.
23. Polli, D., et al., Conical Intersection Dynamics of the Primary Photoisomerization Event in Vision. *Nature* **2010**, *467*, 440-443.
24. Levine, B. G.; Martinez, T. J., Isomerization through Conical Intersections. *Annu. Rev. Phys. Chem.* **2007**, *58*, 613-634.
25. Zietz, B.; Blomgren, F., Conical Intersection in a Bilirubin Model - a Possible Pathway for Phototherapy of Neonatal Jaundice. *Chem. Phys. Lett.* **2006**, *420*, 556-561.
26. Zietz, B.; Macphersona, A. N.; Gillbro, T., Resolution of Ultrafast Excited State Kinetics of Bilirubin in Chloroform and Bound to Human Serum Albumin. *Phys. Chem. Chem. Phys.* **2004**, *6*, 4535-4537.
27. Venkatramaiah, N.; Kumar, G. D.; Chandrasekaran, Y.; Ganduri, R.; Patil, S., Efficient Blue and Yellow Organic Light-Emitting Diodes Enabled by Aggregation-Induced Emission. *ACS Appl. Mater. Interfaces* **2018**, *10*, 3838-3847.
28. He, Z.; Ke, C.; Tang, B. Z., Journey of Aggregation-Induced Emission Research. *ACS Omega* **2018**, *3*, 3267-3277.

29. Li, G. F.; Magana, D.; Dyer, R. B., Direct Observation and Control of Ultrafast Photoinduced Twisted Intramolecular Charge Transfer (TICT) in Triphenyl-Methane Dyes. *J. Phys. Chem. B* **2012**, *116*, 12590-12596.
30. El-Zohry, A. M.; Karlsson, M., Gigantic Relevance of Twisted Intramolecular Charge Transfer for Organic Dyes Used in Solar Cells. *J. Phys. Chem. C* **2018**, *122*, 23998-24003.
31. Roca-Sanjuán, D.; Olaso-González, G.; González-Ramírez, I.; Serrano-Andrés, L.; Merchán, M., Molecular Basis of DNA Photodimerization: Intrinsic Production of Cyclobutane Cytosine Dimers. *J. Am. Chem. Soc.* **2008**, *130*, 10768-10779.
32. Debnath, T.; Maity, P.; Lobo, H.; Singh, B.; Shankarling, G. S.; Ghosh, H. N., Extensive Reduction in Back Electron Transfer in Twisted Intramolecular Charge-Transfer (TICT) Coumarin-Dye-Sensitized TiO_2 Nanoparticles/Film: A Femtosecond Transient Absorption Study. *Chem. Eur. J.* **2014**, *20*, 3510-3519.
33. Yushchenko, O.; Villamaina, D.; Sakai, N.; Matile, S.; Vauthey, E., Comparison of Charge-Transfer Dynamics of Naphthalenediimide Triads in Solution and Π-Stack Architectures on Solid Surfaces. *J. Phys. Chem. C* **2015**, *119*, 14999-15008.
34. Lakowicz, J. R., *Principles of Fluorescence Spectroscopy*; Springer, 2007.
35. El-Zohry, A. M.; Zietz, B., Concentration and Solvent Effects on the Excited State Dynamics of the Solar Cell Dye D149: The Special Role of Protons. *J. Phys. Chem. C* **2013**, *117*, 6544-6553.
36. Wurthner, F.; Kaiser, T. E.; Saha-Moller, C. R., J-Aggregates: From Serendipitous Discovery to Supramolecular Engineering of Functional Dye Materials. *Angew. Chem. Int. Edit.* **2011**, *50*, 3376-3410.
37. Sabate, R.; Estelrich, J., Determination of the Dimerization Constant of Pinacyanol: Role of the Thermochromic Effect. *Spectrochim. Acta A* **2008**, *70*, 471-476.
38. Qin, A.; Jim, C. K.; Tang, Y.; Lam, J. W.; Liu, J.; Mahtab, F.; Gao, P.; Tang, B. Z., Aggregation-Enhanced Emissions of Intramolecular Excimers in Disubstituted Polyacetylenes. *J. Phys. Chem. B* **2008**, *112*, 9281-9288.
39. Luo, J.; Xie, Z.; Lam, J. W.; Cheng, L.; Chen, H.; Qiu, C.; Kwok, H. S.; Zhan, X.; Liu, Y.; Zhu, D., Aggregation-Induced Emission of 1-Methyl-1, 2, 3, 4, 5-Pentaphenylsilole. *Chem. Comm.* **2001**, 1740-1741.
40. Gilani, A. G.; Moghadam, M.; Hosseini, S. E.; Zakerhamidi, M. S., A Comparative Study on the Aggregate Formation of Two Oxazine Dyes in Aqueous and Aqueous Urea Solutions. *Spectrochim. Acta A* **2011**, *83*, 100-105.
41. Arbeloa, F. L.; Ojeda, P. R.; Arbeloa, I. L., Dimerization and Trimerization of Rhodamine 6g in Aqueous-Solution - Effect on the Fluorescence Quantum Yield. *J. Chem. Soc. Farad. T. 2* **1988**, *84*, 1903-1912.
42. Satchell, D. P.; Wardell, J. L., Dimerization of Carboxylic Acids in O-Dichlorobenzene. *T. Farad. Soc.* **1965**, *61*, 1199-&.
43. El-Zohry, A. M., The Origin of Slow Electron Injection Rates for Indoline Dyes Used in Dye-Sensitized Solar Cells. *Dyes Pigm.* **2019**, *160*, 671-674.
44. Hussain, M.; El-Zohry, A. M.; Gobeze, H. B.; Zhao, J. Z.; D'Souza, F.; Mohammed, O. F., Intramolecular Energy and Electron Transfers in Bodipy Naphthalenediimide Triads. *J. Phys. Chem. A* **2018**, *122*, 6081-6088.
45. Dereka, B.; Koch, M.; Vauthey, E., Looking at Photoinduced Charge Transfer Processes in the Ir: Answers to Several Long-Standing Questions. *Acc. Chem. Res.* **2017**, *50*, 426-434.

46. Zhong, D. P., Electron Transfer Mechanisms of DNA Repair by Photolyase. *Annu. Rev. Phys. Chem.* **2015**, *66*, 691-715.
47. Messina, F.; El-Zohry, A. M.; Mohammed, O. F.; Chergui, M., The Role of Site-Specific Hydrogen Bonding Interactions in the Solvation Dynamics of N-Acetyltryptophanamide. *J. Phys. Chem. B* **2012**, *116*, 10730-10738.
48. Zhang, W. Q.; Li, Q. Y.; Cheng, J. Y.; Cheng, K.; Yang, X. Y.; Li, Y. W.; Zhao, X. S.; Wang, X. J., Ratiometric Luminescent Detection of Organic Amines Due to the Induced Lactam-Lactim Tautomerization of Organic Linker in a Metal-Organic Framework. *ACS Appl. Mater. Interfaces* **2017**, *9*, 31352-31356.
49. Mostakim, S. K.; Biswas, S., A Thiadiazole-Functionalized Zr(IV)-Based Metal-Organic Framework as a Highly Fluorescent Probe for the Selective Detection of Picric Acid. *Crystengcomm* **2016**, *18*, 3104-3113.
50. Neto, B. A. D.; Carvalho, P. H. P. R.; Correa, J. R., Benzothiadiazole Derivatives as Fluorescence Imaging Probes: Beyond Classical Scaffolds. *Acc. Chem. Res.* **2015**, *48*, 1560-1569.
51. Feng, S.; Li, Q. S.; Yang, L. N.; Sun, Z. Z.; Niehaus, T. A.; Li, Z. S., Insights into Aggregation Effects on Optical Property and Electronic Coupling of Organic Dyes in Dye Sensitized Solar Cells. *J. Power. Sour.* **2015**, *273*, 282-289.
52. Sabate, R.; Gallardo, M.; de la Maza, A.; Estelrich, J., A Spectroscopy Study of the Interaction of Pinacyanol with N-Dodecyltrimethylammonium Bromide Micelles. *Langmuir* **2001**, *17*, 6433-6437.
53. El-Zohry, A. M.; Cong, J.; Karlsson, M.; Kloo, L.; Zietz, B., Ferrocene as a Rapid Charge Regenerator in Dye-Sensitized Solar Cells. *Dyes Pigm.* **2016**, *132*, 360-368.

TOC Graphic

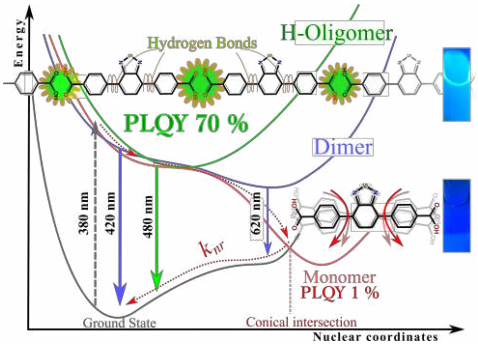
Energy
Hydrogen Bonds
H-Oligomer
PLQY 70 %
Dimer
380 nm
420 nm
480 nm
620 nm
k_{nr}
Monomer
PLQY 1 %
Ground State
Conical intersection
Nuclear coordinates